ACS APPLIED MATERIALS & INTERFACES

Biological and Medical Applications of Materials and Interfaces

Nano-Protrusive Gold Nanoparticle Hybridized Polymer Thin Film as A Sensitive, Multi-Patternable and Antifouling Biosensor Platform

Jeong-Hoon Lee, Byung-Soo Park, Hyun-Gu Ghang, Hyunjoon Song, and Sung Yun Yang

ACS Appl. Mater. Interfaces, **Just Accepted Manuscript** • DOI: 10.1021/acsami.8b03681 • Publication Date (Web): 04 Apr 2018

Just Accepted

ACS Publications

is published by the American Chemical Society. 1155 Sixteenth Street N.W., Washington, DC 20036

Nano-Protrusive Gold Nanoparticle Hybridized Polymer Thin Film as A Sensitive, Multi-Patternable and Antifouling Biosensor Platform

*Jeong-Hoon Lee†,§, Byung-Soo Park†,§, Hyun-Gu Ghang†, Hyunjoon Song‡, Sung Yun Yang†,**

† Department of Polymer Science and Engineering, Chungnam National University, 99 Daehak-Ro, Yuseong-gu, Daejeon 34134, Republic of Korea.

‡ Department of Chemistry, Korea Advanced Institute of Science and Technology, 291 Daehak-Ro, Yuseong-Gu, Daejeon 34141, Republic of Korea.

KEYWORDS: Polyelectrolyte, Anisotropic gold, nano-protrusive particle, antifouling, biosensor

ABSTRACT: Hybrid films consisting of anisotropic octahedral gold nanoparticles and polymers had their surfaces functionalized and were immobilized on surface plasmon resonance (SPR) sensors for biomolecule detection. Specifically, carboxylated octahedral gold nanoparticles (C-Oh-AuNPs) and poly(allylamine hydrochloride) (PAH) were assembled as ultrathin films by using layer-by-layer process. The ionic strength generated from the functional groups of C-Oh-AuNP and PAH influenced the composition, its surface morphology, and the reactivity of the film toward further chemical reactions such as the synthesis of spherical AuNPs (S-AuNPs). We were thus able to control the size and the structure of the C-Oh-AuNP and S-AuNPs converted to

nano-raspberry shape particles. This hierarchical AuNP hybrid film exhibits much more sensitive and stable detection of biomolecules than regular flat chip systems, and this result may be due to the SPR of the AuNP at its surface being able to markedly enhance the local optical field of the chip. The micro-patterning of the hybrid coating was also studied by using a soft lithographic patterning method. We in particular worked on creating multiplex patterns having different combinations of shapes and fluorescent colors. We expect our hybrid coating system with multi-code biomolecular arrays to be used as a powerful platform for biosensor applications.

INTRODUCTION

Gold exhibits many attractive properties, such as high stability and biocompatibility, the ability to form various shapes in various sizes, and strong electrical or optical properties.[1, 2] In particular, the optical properties of gold nanoparticle (AuNP) are of great interest for nanoscale research and applied sensing applications.[3, 4] The fabrication of three-dimensional arrays of AuNPs on flat substrates or thin films can be employed to tune and manipulate their optical properties.[5] This type of fabrication also allows for characterization using surface-sensitive spectroscopic and microscopic analytical methods. Because the excitation of surface plasmon resonance (SPR) can greatly enhance the local optical field, these films also have the potential for applications as sensors.[6-9] SPR of gold is affected not only by the size of the gold particle but also by its shape, so recent studies have focused on synthesis of anisotropic gold particles such as nanoprisms, nanorods and nanosheets.[9-14] Addition to the interesting properties of gold nanoparticles, many synthetic routes of controlled gold synthesis might be the reason to keep this research field continuously growing. The most widely used synthesis of shape-controlled AuNPs may be catalytic solution-based synthesis.[9-13] For example, tetrahedral, cubic, or octahedral gold

nanoparticles can be synthesized in the reaction of auric acid aqueous solution in the presence of citric acid and amine group-containing polymer, such as poly(vinylpyrrolidone), within a batch reactor based on pH and/or temperature to control the nucleation and growth process of gold. [9-10]

Sputter deposition is also versatile technique for metal nanoparticle synthesis, which can readily control the properties of organic-inorganic nanocomposites by monitoring their composition and manipulating the arrangement of atoms without chemical purification and synthesis.[15] In recent studies of sputtering, in-situ growth of metal thin films from small islands over fractal gold cluster arrangement was conducted and demonstrated how specimen properties correlate with the nanoparticle size, shape and interfacial morphology of the deposited metal layer. Especially, Schwartzkopf et. al. reported a highly controllable sputtering method that a variation of deposition rate could affect the average interparticle distances and growth morphology to tailor polymer-metal-nanocomposites resulting in hierarchical structured materials which can be useful for sensing applications.[16-17]

Despite the many advantageous properties and established synthetic methods of gold nanoparticles, the control of the modification of gold nanoparticles is often insufficient to use them for many applications. Especially, modifying particle surfaces with organic or biochemical components with the suitable stability and the functionality for specific recognition in sensing technology is still not easily achieved. One of the most well established modification to introduce biochemical com-pounds onto gold surface is the conjugation reaction using active terminal groups such as thiol group, however, the bioactivity of the biomolecule bound by this method is not well retained. Therefore, it is required to finding a system for enhanced stability of the bioactive molecule immobilization by mimicking biochemical environment.

We have successively synthesized various inorganic nanoparticles and functionalized with nanostructured poly-electrolyte multilayer films as reaction templates.[18-19] The multilayer films were prepared by layer-by-layer (LbL) process which is a fabrication method to coat a substrate by dipping the substrate stepwise into dilute polymer solutions in which electrostatic or hydrogen-bonding interactions between the polymers exist.[20] The film coated by this technique is especially useful in the further modification such as bio-conjugation, micro-patterning, or metal particle hybridization. [21-26]

In the current work, we used anisotropic octahedral gold nanoparticles and functionalized their surfaces with car-boxyl groups for the hybrid film study, denoted as C-Oh-AuNPs. These C-Oh-AuNPs were immobilized using the amine-functionalized polymer, poly(allylamine hydrochloride) (PAH), on an SPR sensor chip for biomolecule detection. These hybridized films consisting of C-Oh-AuNPs and PAH were deposited on the substrate by carrying out LbL deposition. C-Oh-AuNP and PAH interacted ionically, and the strengths of these ionic interactions were changed by varying the pH conditions of their solutions in order to obtain different deposition properties. The optical properties of the AuNP arrays were controlled by changing the quantity and distribution of the AuNPs. Our multilayer AuNP hybrid coating provided a greater sensitivity for biomolecule detection than has been shown for the regular SPR chip system. Especially, we created a hybrid coating system with hierarchical nanostructured AuNPs having "nano-raspberry" shape, several nanometer-sized Au nanodots attached on an octahedral Au nanoparticle, exhibited the sharper and larger signals in bio-sensing experiments.

Additionally, we created micro-patterned AuNP arrays of functionalized C-Oh-AuNPs on polymer films. Micro-patterning of polymer films has been used to fabricate bio-active arrays.[27-30] Here we built stepwise complex patterns, consisting of shape- and color-indexed spots.

Different biomolecules bound to patterns with different shapes, which enabled the determination of which biomolecule was anchored to which sensor, even if the same fluorescent probe was used and multiple biomolecules were sensed. To improve the ability of the C-Oh-AuNPs to detect biomolecules, we tested various concentration and pH conditions. We also tried to detect biomolecules by taking SPR measurements and applying patterning by using poly(dimethyl siloxane) (PDMS) stamp[31] with polymer solution as an ink. [32-33] The results of our experiments showed the versatile potentials of the C-Oh-AuNPs/polyelectrolyte hybrid system to be applied as biosensors.

EXPERIMENTAL

Materials: Weak polyelectrolytes including poly(allylamine hydrochloride) (PAH) (MW = 60,000), poly(acrylic acid) (PAA) (MW = 90,000), poly(methacrylic acid) (PMA) (MW = 100,000) and polyacrylamide (PAAm) (MW = 5,000,000) were purchased from Polysciences. Carboxylated octathedral gold nanoparticles(C-Oh-AuNPs) were synthesized by the method of Song et al.[9-10] Hydrogen tetrachloroaurate(□) trihydrate (HAuCl4• $3H_2O$) (Sigma Aldrich) and dimethylamine-borane complex (DMAB) (Sigma Aldrich) were used to synthesize spherical AuNPs in the film. Dulbecco's Modified Eagle's medium (DMEM) and trypan blue were purchased from Sigma Aldrich. Immunoglobulin G (IgG) from human serum, anti-Rabbit IgG produced in goat, PSA and anti-PSA were purchased from Sigma Aldrich. Streptavidin, sulfo-succinimidyl 6-[3'-(2-pyridyldithio)-propionamido] hexanoate (sulfo-LC-SPDP) and dithiothreitol (DTT) were purchased from Thermo Fisher Scientific. For the dual color micro-patterning experiment, TRITC-labeled IgG antibody (TRITC-anti-Rabbit IgG) and biotin-fluorescein were purchased form Sigma.

Deposition of polyelectrolyte multilayer (PEM) films: The carboxylated octahedral gold nanoparticles (C-Oh-AuNPs) and PAH multilayers were assembled by using the layer-by-layer (LbL) deposition method. Specifically, PAH/C-Oh-AuNP multilayers were assembled on various substrates, including glass, silicon and surface plasmon resonance (SPR) gold substrates, by sequentially dipping the substrate into a dilute aqueous solution of the PAH polycation and a dispersed suspension of ionized C-Oh-AuNP, resulting in the sequential adsorption of PAH and C-Oh-AuNP onto the substrate. Slide glasses and silicon substrates were used for measuring the ultraviolet-visible (UV-Vis) absorbance of the gold in order to determine the thickness of the film. Each SPR substrate was cleaned with a piranha solution for a minute followed by being rinsed with de-ionized water using an ultrasonic cleaner. The other substrates were washed with a detergent (MICRO®-sol) and de-ionized water with sonication. After cleaning, the substrates were blow dried with N_2 gas and cleaned by plasma cleaner (Harrick Plasma, PDC-32G) for one minute under vacuum prior to the dipping. Polymer solutions were prepared with a concentration of 0.01 M based on the molecular weight of the repeating unit. Aqueous hydrochloric acid (HCl) and potassium hydroxide (KOH) solutions were used to adjust the pH of the dipping solution. The pH of the PAH solution was adjusted to 8.5, and that of the Oh-AuNP solution to 8.5 and 6.0. De-ionized water (~18 MΩ cm) was used to prepare all aqueous solutions and for all rinsing steps. The substrate was immersed into the PAH aqueous solution for 15 minutes followed by a 2 min rinsing with water and agitation. The rinsing step was repeated at least 2 times. The substrate to which the PAH was adsorbed was then dipped into the C-Oh-AuNP dispersed solution with stirring for 15 min. After this step, the above-described rinsing process was applied again. This process was repeated until a desirable film thickness was obtained.

Morphological and surface charge characterization the C-Oh-AuNP and C-Oh-AuNP/PAH films: The resulting film morphology was examined using a Park System XE-200 atomic force microscope (AFM) and a JEOL (model JSM-7000F) scanning electron microscope (SEM). Zeta potential was measured by particle size analyzer by Malvern (model: Zeta sizer nano zs).

Thermal crosslinking: In order to increase the stability of the PAH/Oh-AuNP hybrid film from swelling in buffered solution where the antibody conjugation and antigen detection reaction will take a place, the hybrid film was thermally crosslinked at 120 ^{o}C for 3 h in a vacuum oven.

In-situ synthesis of hierarchical gold nanoparticle system: To synthesizing spherical AuNPs using hybrid multilayer film, three types of hybrid films were prepared. One is direct deposition of C-Oh-AuNP with PAH, i.e. (PAH/C-Oh-AuNP)n, another is mixed system of PAH/C-Oh-AuNP and PAH/PAA, i.e. [(PAH/C-Oh-AuNP) + (PAH/PAA)]n, and the other is [(PAH/C-Oh-AuNP)1 + (PAH/PAA)3]n system. The pH conditions of (PAH/C-Oh-AuNP) and (PAH/PAA) are 8.5/6.0 and 8.5/3.5, respectively. These hybrid films were each immersed into a HAuCl4 (5 mM) solution for 5 min, to allow the gold ions to bind the carboxyl functional groups of C-Oh-AuNP, and then rinsed twice with de-ionized water, each time for two minutes. The resulting films were each immersed into a reduction bath (aqueous solution of 5 mM borane-dimethyl amine, DMAB) for 5 min and then rinsed with de-ionized water twice. The resulting S-AuNP-synthesized multilayer films were examined by using a UV-Vis spectrometer and scanning and scanning electron microscopes (JEOL, model JSM-7000F).

Antibody immobilization and SPR measurements: IgG and PSA antibodies were immobilized in the polymer/gold nanoparticle-hybridized porous coating on an SPR chip for detecting. Each step related to the hybrid film deposition and antibody immobilization was monitored by using an

SPR instrument (model: SPR Lab, K-MAC) in its static mode. Antigen binding event, for the comparison between PAH/C-Oh-AuNP hybrid and hierarchical PAH/AuNP-hybrid films coated chip on antigen detection, was studied by an additional SPR instrument manufactured by Biacore Co (at Nanofab at KAIST). The thiol-activated cross-linker used to immobilize anti-IgG onto the gold surfaces was prepared by conjugating sulfo-LC-SPDP. For the antigen detection experiment, IgG was made to flow on the modified SPR chip. When the real-time experiments were con-ducted, PBS buffer solution was first injected in the channel at a flow rate of 20 μl per minute until the baseline was stabilized. After the signal was stable, antigen was injected. After the signal was stable, a volume of 300 μl of 0.67 μm antigen was injected into the channel at a flow rate 5 μl per minute. A PBS buffer solution was delivered into the chamber again, when the antigen injection was finished, in order to rinse off any unbound antigen from the chip.

RESULTS AND DISCUSSION

Surface Modification of Anisotropic Gold Nanoparticles and Composite Film Formation by Layer-by-layer Process

We used LbL deposition procedure to introduce anisotropic AuNPs on the biomolecular sensing chip. The AuNPs were synthesized by carrying out a solution-catalyzed reduction of an Au ion-containing solution in the presence of poly(vinyl pyrrolidone). The structures of the AuNPs used in this study were shown to be octahedral and their surfaces were modified by carboxylate groups, negative charges built up on the nanoparticles. Therefore, these AuNPs, denoted as C-Oh-AuNPs, were assembled using ionic interactions with a polyelectrolyte, PAH, consisting of cationic side chains and were then deposited as multilayer films on substrates by

using the LbL method. We followed a typical LbL procedure, which was previously published elsewhere.[18]

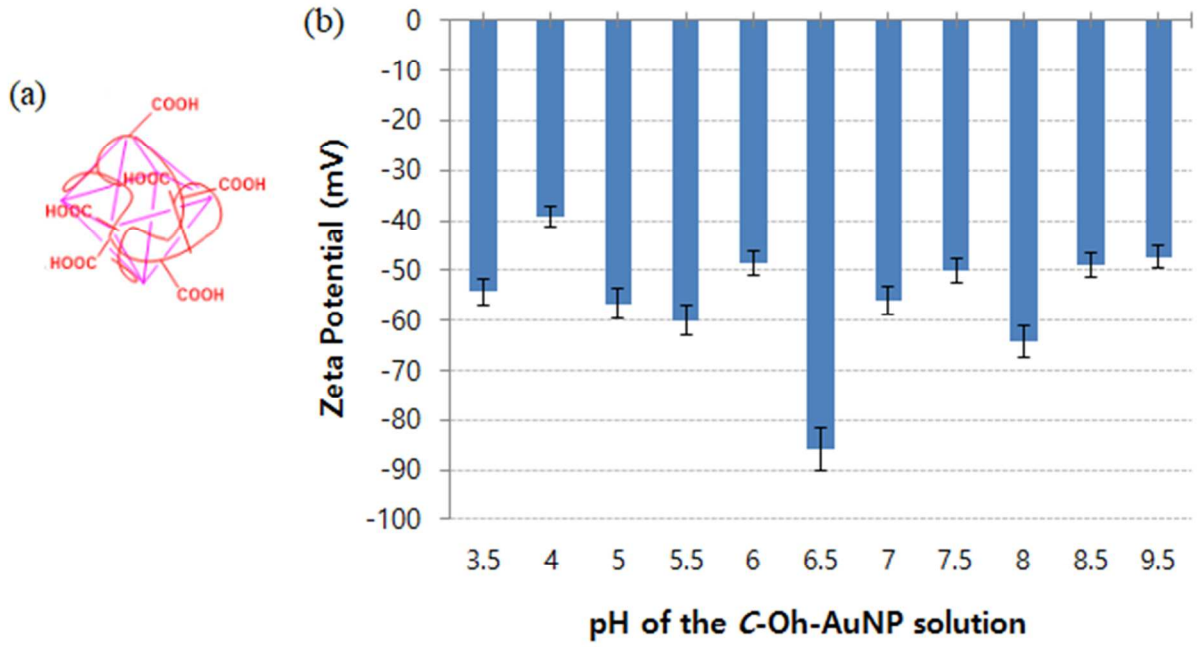

Figure 1. (a) Schematic view of a C-Oh-AuNP and (b) Zeta potentials of the diluted the C-Oh-AuNP dipping solutions prepared at various pH conditions.

Since the amine groups of PAH and the carboxyl groups of C-Oh-AuNP can be ionized to various extents, as is characteristic of weak electrolytes, we carefully considered the pH conditions of the C-Oh-AuNP suspended solution as well as of the PAH aqueous solution in the dip-coating process. At first, the surface zeta potentials of C-Oh-AuNPs suspended in de-ionized water at various pH conditions were studied (**Figure 1**). The C-Oh-AuNPs in the pH range 6.0~8.5 exhibited the highest surface charges while pH below 5.0 or higher than 9.0 seemed not good enough for effective ionization of the carboxyl groups on AuNPs.

We tried to make the multilayer films of the PAH/C-Oh-AuNP assembly at various pH conditions. For the film deposited on a flat substrate (for example, a glass slide or silicon wafer), the substrate was initially covered with a layer of cationic PAH since the residual negative charge of the substrate might interact strongly with cationic molecules. Therefore, the C-Oh-AuNP was deposited onto the PAH-coated substrate afterward. Because SPR measurements cannot be taken from films thicker than a certain value, we needed to optimize the thickness of the PAH/C-Oh-AuNP coating for the SPR chip. By tuning the pH conditions of the PAH and C-Oh-AuNP dipping solutions, the film composition and thickness were changed (**Figure 2**).

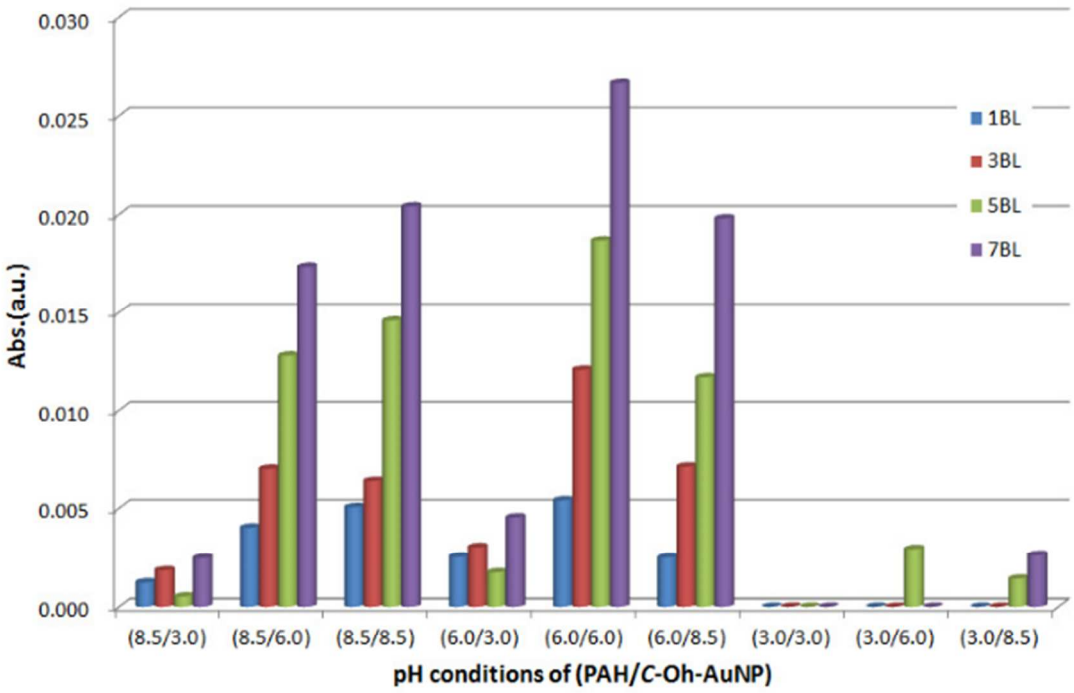

Figure 2. The quantities of C-Oh-AuNPs in the PAH/C-Oh-AuNP-hybridized multilayer films for various pH values of the dipping solutions and for various numbers of layers, as derived from UV absorbance measurements.

The UV-visible absorption spectra of the PAH/C-Oh-AuNP films were acquired and indicated that the quantity of C-Oh-AuNPs in the deposited hybrid film proportionally increased with the number of bilayer repeating cycles.

Based on the surface charge result, we expected to make successful multilayer films of the PAH/C-Oh-AuNP at pH 3.0 ~ 6.0 for PAH and 6.0 ~ 8.5 for C-Oh-AuNP where the ionization of two components are larger than 50%. This turned out mainly true as we obtained the results summarized in Figure 2. The fastest increase in the film thickness was observed when using pH values of 6.0 ~ 8.5 for the PAH/C-Oh-AuNP dipping solutions. We also measured the surface morphology of the PAH/C-Oh-AuNP films, which the films were assembled with different pH condition of the C-Oh-AuNPs at constant pH for PAH. As seen by AFM images, the more C-Oh-AuNP particles were assembled at high pH condition, 6.0 and 8.5, compared to pH 3.0 (**Figure 3**). This is probably due to the incremental electrostatic interaction between negatively charged COO- groups of C-Oh-AuNP and positive NH_3^+ groups of PAH.

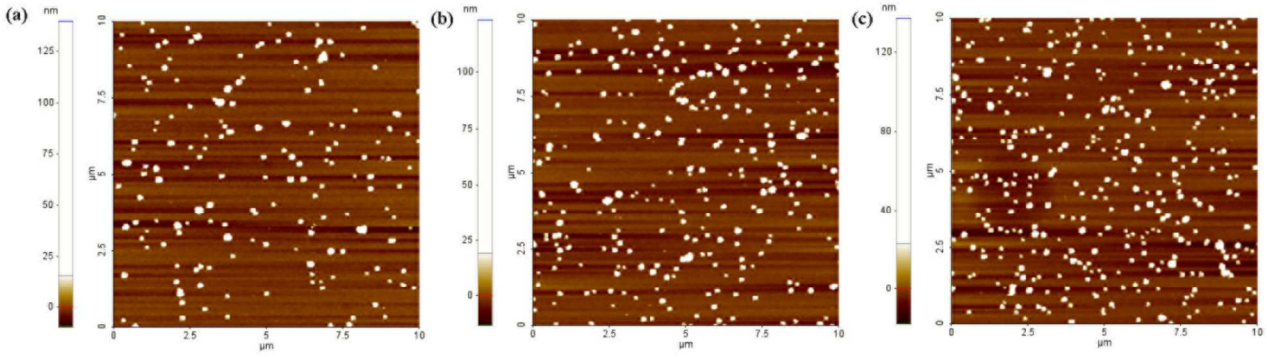

Figure 3. AFM images revealed the distribution of the assembled C-Oh-AuNPs in PAH/C-Oh-AuNP hybrid multilayer films corresponding to the dipping solution pH conditions. pH of the C-Oh-AuNPs solution was controlled as (a) 3.0, (b) 6.0, (c) 8.5 and the pH of PAH was 8.5.

Biomolecular Sensing of an SPR Chip Coated with a PAH/C-Oh-AuNP Hybrid Film

We studied the protein sensing ability of the PAH/C-Oh-AuNP films by using their SPR characteristics. A gold thin layer-sputtered chip was used for the measurement. In order to enhance the adhesion of the film onto the chip, we applied the (PAH/PAA) one layer prior to

applying the (PAH/C-Oh-AuNP) film. However, due to the instrumental limitations regarding the thickness of the film on the SPR chip (only up to 100~120 nm, even much less with high refractive index material), we could apply only a few bilayers of the PAH/C-Oh-AuNP hybrid film.

Below **Figure 4** shows the surface plasmon resonance (SPR) signals obtained from the hybrid film coated sensor chips versus a regular non-coated sensor chip. The SPR sensor chip consisted with thin metal gold film deposited on prism and we coated PAH/C-Oh-AuNP hybrid film atop of it. The surface plasmon angle (θ_{sp}) corresponds to the sine function of the dielectric constants of metal gold (ε_m), prism (ε_p), and coated layer on the metal surface (ε_l) based on the equation 1 listed below. Refractive index of layer, n_l, correlates to the amount of the coated layer (ε_l). As PAH and C-Oh-AuNP is coated on the metal surface, the more SPR angle shift, $\Delta\theta$, can be observed.

$$\theta_{sp} = sin^{-1}\sqrt{\frac{\varepsilon_l\,\varepsilon_m}{(\varepsilon_l+\varepsilon_m)\varepsilon_p}}\ ,\ n_s = \sqrt{\varepsilon_l} \text{--------- eq. 1}$$

Using the spectral static mode of SPR, we checked each sequential step of the PAH/C-Oh-AuNP-coated SPR chips (**Figure 4a**). As the first step of the coating, 1.5 bilayers of PAH/PAA (about 15 nm thick) were deposited as an adhesion-supporting layer for the bare chip and the SPR angle shifted from 53.0˚ to 53.5 ˚. Then, as following deposition step of C-Oh-AuNPs the SPR angle (θ_{sp}) increased to 54.75 ˚. In the case of reflectance, it drastically changed from 6.5 % to 23.2 %, as yielding Δn to be 16.7%, corresponding to the heavier component (gold particles) than the case of polymer. This is a big change of SPR with only one layer of gold particles compared to the previous study of AuNPs with polyelectrolytes reported by Advincula's group.[5]

They provided a profound analytical study of the polyelectrolyte/AuNP multilayer film including swelling behavior on pH changes by using both experimental data and theoretical calculation. The AuNPs in their system are just simple spherical nanoparticles and therefore, the SPR absorption peak of the deposited film monotonously increased as the number of layers increased. Our anisotropic gold nanoparticles (C-Oh-AuNPs) exhibit much higher increase in refractive index compared with the spherical AuNPs. Besides, the chemical functional groups of the C-Oh-AuNP can be utilized for any further modification. Therefore, we applied antibody (anti-IgG) conjugation to the C-Oh-AuNP coated film (**Figure 4b~d**).

When we tested antibody-antigen binding using a microfluidic SPR sensor, found the hybrid coating needed to be partially cross-linked in order to perform reliable signaling. Otherwise, very unstable signal would be observed (**Figure 4b**). So, thermally induced crosslinking between carboxylic acid and amine functional groups in the film was conducted before antibody conjugation at 90^{o}C for 6 h and the reaction confirmed by FT-IR similar to our prior arts. During antibody conjugation and antigen detection the coated hybrid film must be exposed to a phosphate buffered saline (PBS) solution at pH 7.4. At this condition (high pH with salts), the AuNP/polyelectrolyte hybrid film is considered in a highly swollen state, and it may cause some deformation or delamination of the coating. Therefore, we modified the hybrid film lightly cross-linked (5~7% amide links between PAH and C-Oh-AuNP in FR-IR) prior to the antibody conjugation step.

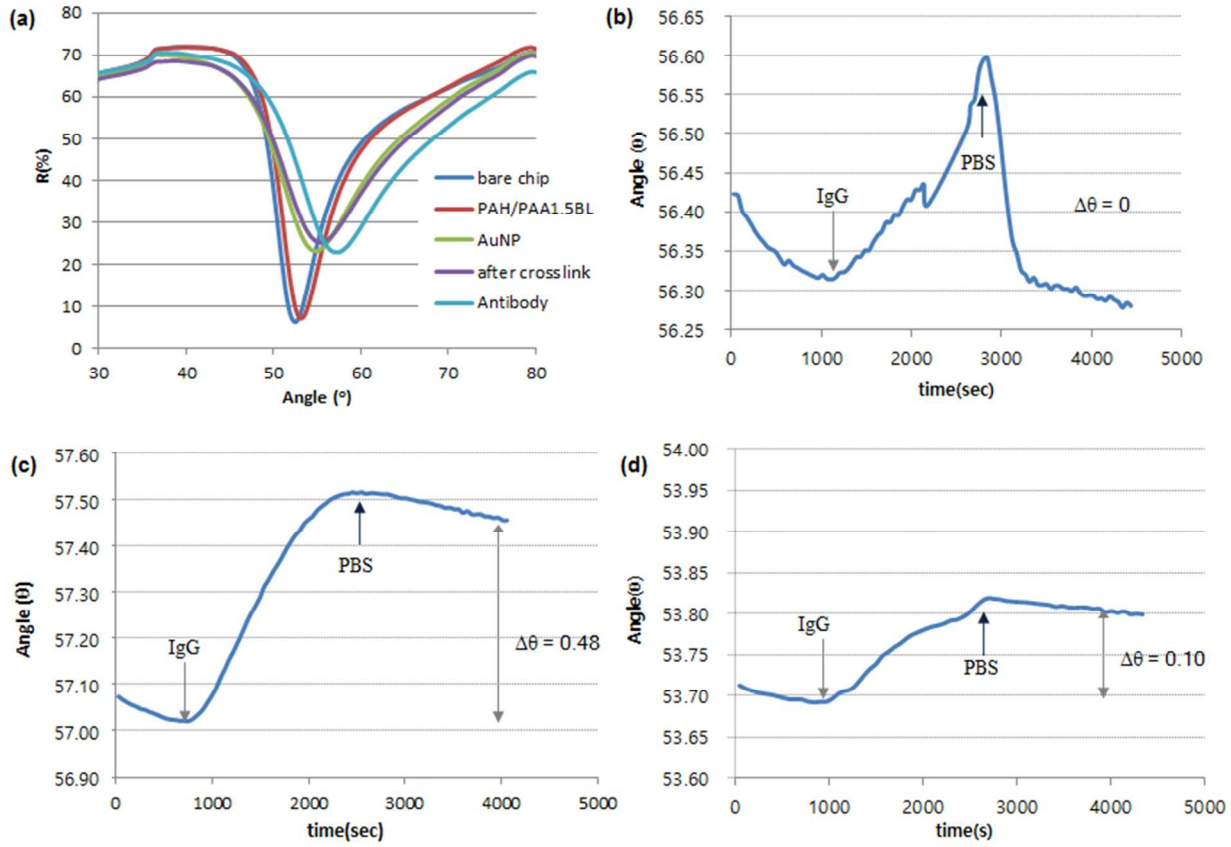

Figure 4. SPR analysis of the AuNP-polyelectrolyte multilayer films and IgG antigen sensing. Spectral static mode (reflectance-vs-incident angle plot) was used for (a) stepwise SPR spectra of the (PAH/C-Oh-AuNP)-coated gold chip (R: % reflectance). Detection of IgG in real time SPR angle (θ) mode using anti-IgG immobilized (PAH/C-Oh-AuNP)-coated chips; (b) without crosslinking (c) with crosslinking of the hybrid coating film. For the comparison, (d) immobilized anti-IgG on a regular bare gold chip was studied. The pH condition of (PAH/C-Oh-AuNP) assembly is 8.5/6.0. The amount of captured IgG corresponding to angle shift is approximately as 0.1 degree ≈ 1 ng/mm^2.

After crosslinking of the hybrid film, the SPR angle and the reflectance of the film were slightly increased to 55.0˚ and 25.4%, respectively. These changes might be only from the film densification because there was no addition of new material related to. Upon immobilizing anti-IgG on the PAH/C-Oh-AuNP coating, the SPR angle greatly in-creased from 55.0˚ to 57.3˚,

reflecting an effective conjugation of the antibody to the coating. This increased amount ought to be emphasized considering it is from only a single layer of C-Oh-AuNPs. Finally, detection of antigen binding was recorded in real time mode by using a fluidic SPR sensor. This detection was accomplished by fabricating biochips using the AuNP hybrid film coated on gold chip where antibodies were immobilized. Compared to a flat SPR chip (**Figure 4d**), this hybrid coating chip has the higher surface/volume ratio and expresses the stronger binding signals (**Figure 4c**). This increased surface/volume ratio was shown to be suitable for detecting relatively un-stable bio-active components.

Creating Hierarchical AuNPs System: Raspberry-shape Nano-protrusive AuNPs Prepared by In-situ Synthesis of Spherical AuNPs (S-AuNPs) on the Surface of C-Oh-AuNPs

As discussed above, we obtained enhanced SPR spectroscopic absorbance from C-Oh-AuNP containing film com-pared to regular flat chip. However, due to the thickness limitation of the surface coating for SPR sensor we could not increase the detection sensitivity by increasing the amount of C-Oh-AuNP in the coating. Therefore, we de-signed a new hybrid film system having the additional AuNPs utilizing the functionality of C-Oh-AuNP and poly-electrolytes that were assembled as mixed AuNP-PEM films. The mixed AuNP-PEM films were prepared with PAH/C-Oh-AuNP and PAH/PAA sandwiched multilayers. Then we performed the in-situ gold nanoparticle synthesis using the sandwiched multilayers as reaction templates. We and others reported the synthetic method for spherical gold nanoparticles by using PAH/PAA multilayers as a reaction template.[18, 34] Ionization level of the chemical functional groups in this weak polyelectrolyte multilayer film was considered as the most important factor for inorganic nanoparticle synthesis while carboxylic acid or amine groups played the singular or concerted initial binding sites of metal salt ions depending on the reaction condition.[19, 35-36] In general, non-

ionized free carboxylic acid and amine groups containing polyelectrolyte multilayer films are considered as the most preferred templates for inorganic particle synthesis.[18-19, 34]

We prepared the sandwiched films of $[(PAH/C\text{-}Oh\text{-}AuNP)_1+(PAH/PAA)_x]n$, where x = 0~3 (film deposition number) and n = 1~7 (repeating number of gold synthesis). The pHs of the multilayers of PAH/C-Oh-AuNP and PAH/PAA were adjusted as 8.5/6.0 and 8.5/3.0 respectively. Prior to nanoparticle synthesis, the PAH/PAA films were treated with a low pH solution to undergo nanoporous transition. Then PAH/PAA multilayer film became having many active binding sites for metal precursor ions. Since the surfaces of the C-Oh-AuNPs as well as PAA display carboxyl functional groups, there are two different reactive spots in this spherical gold nanoparticle synthesis. These two types of spherical gold nanoparticles (S-AuNPs) may represent different optical properties based on the situation where they lied on.

In order to check the optical properties of the films we measured UV absorption spectrum for each sample (**Figure 5**). The maximum UV absorption peak was increased as increasing the layer number of the hybrid films in all three cases, however, higher absorption spectra were obtained from the sandwiched samples, **Figure 5(b~c)** films containing the additional PAH/PAA multilayer, than the PAH/C-Oh-AuNP-only film. In these sandwiched film samples, S-AuNPs might be synthesized from both C-Oh-AuNPs and PAH/PAA sides. Especially, a drastic non-linear increase was observed from (c) which has 1:3 ratio of PAH/C-Oh-AuNPs to PAH/PAA layers.

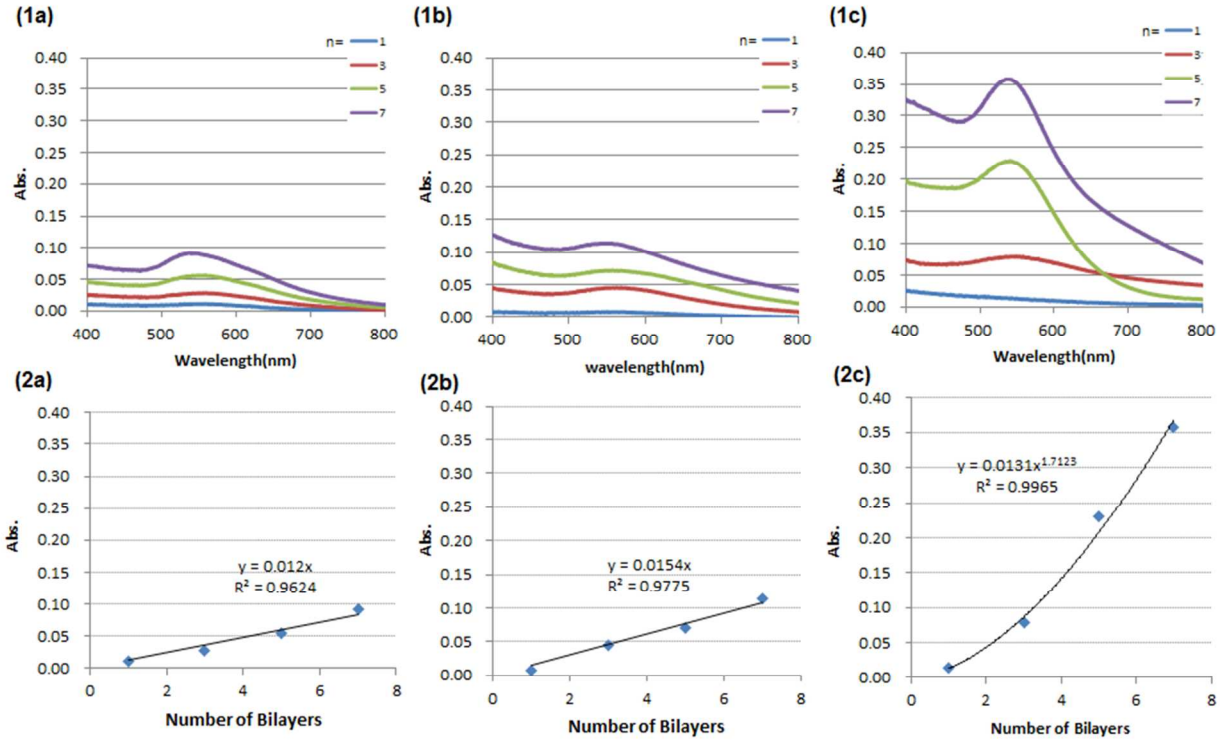

Figure 5. (1) UV absorption spectra of the products of in-situ syn-thesis of S-AuNPs using (a) PAH/C-Oh-AuNP film only, (b) $[(PAH/C\text{-}Oh\text{-}AuNP)_1 + (PAH/PAA)_1]_n$ films and (c) $[(PAH/C\text{-}Oh\text{-}AuNP)_1 + (PAH/PAA)_3]n$ films. (2) Corresponding plots of the functional of layer numbers with the maximum absorbance. (n=1, 3, 5, 7, S-AuNP reaction cycle number).

This exponential growth in SPR absorption of the sample (c) might be caused by other than just increasing of the reactive functional groups in the film; therefore, we studied the morphological property of the sandwiched film. We obtained some microstructures of the three different samples used above by acquiring SEM images (**Figure 6**). These images evidence the successful synthesis of S-AuNPs and a peculiar hierarchical morphology of S-AuNPs conjugated on a C-Oh-AuNP particle. In the PAH/C-Oh-AuNP sample, some of S-AuNPs are in the film surface and others are on the C-Oh-AuNP surface like as a large particle aggregate (**Figure 6a**). Inset images of the same figure show very dis-tinctive morphology of the S-AuNP synthesized on C-Oh-AuNP compared to the bare C-Oh-AuNP. While bare C-Oh-AuNP exhibits a quite

smooth surface with an averaged diameter around 48 nm, after synthesis the C-Oh-AuNP presents many small protrusions on its surface and the diameter increased up to 68 nm. More profound hierarchical structures appeared from the sandwiched [PAH/C-Oh-AuNP + PAH/PAA] films (**Figure 6b**~ 6c).

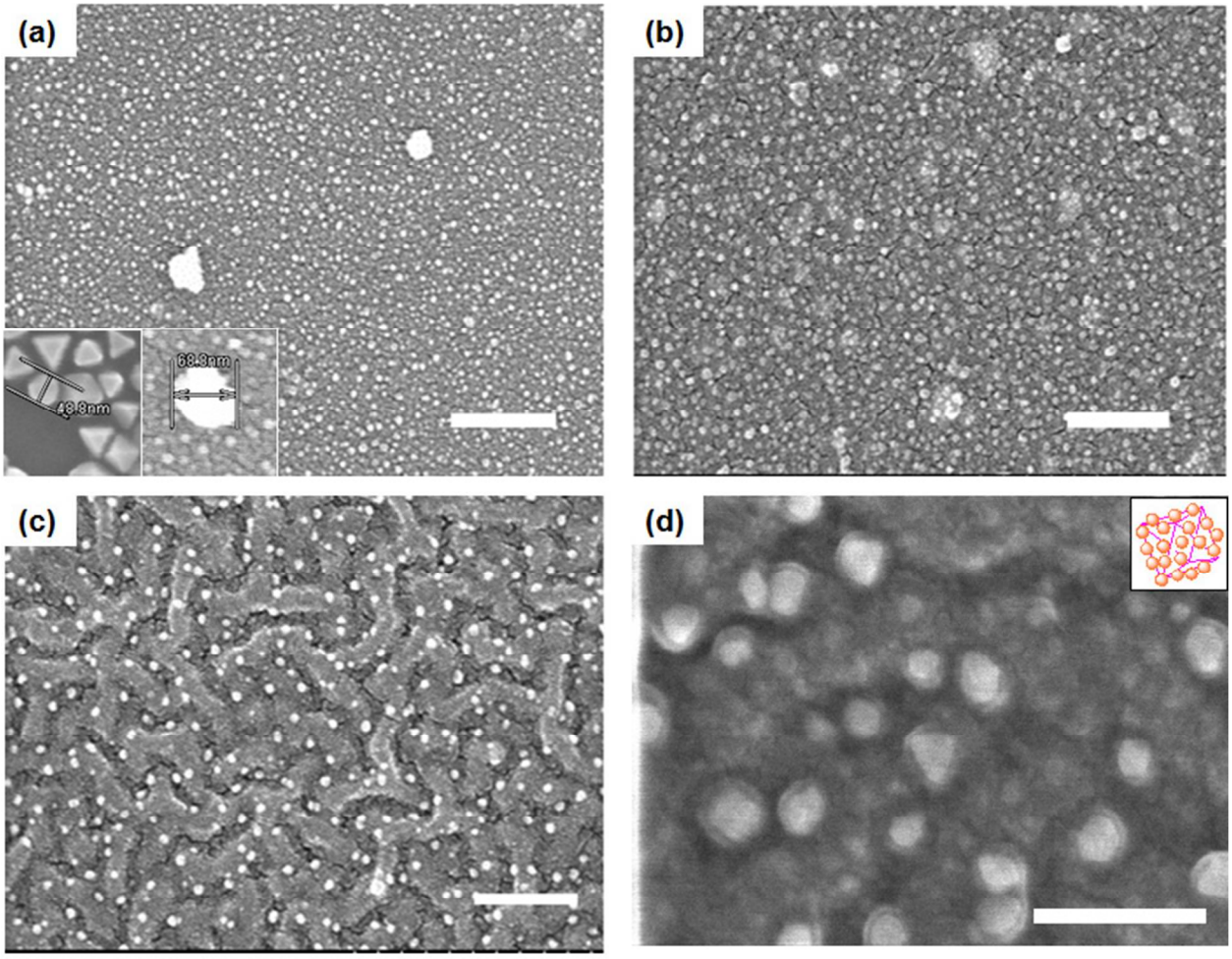

Figure 6. SEM images of the products of in-situ synthesis of S-AuNPs using PAH/C-Oh-AuNP films and PAH/C-Oh-AuNP and PAH/ PAA sandwiched films. Samples were prepared by the reduction of the Au ions bound to the (a) $(PAH/C\text{-}Oh\text{-}AuNP)_3$ film, (b) $[PAH/C\text{-}Oh\text{-}AuNP+ PAH/PAA]_3$ films and (c) $[(PAH/C\text{-}Oh\text{-}AuNP)_1+(PAH/PAA)_3]_3$ films. (d) The closer image of (c) to visualize S-AuNPs on the surface of C-Oh-AuNPs. (Scale bar, 100nm)

Many nano-sized spherical nanoparticles covered on a C-Oh-AuNP with very tight conjugation, looking very similar to raspberries or protrusive surface of a lotus leaf. We denote this protru-sive gold nanoparticle as 'Nano-Raspberry AuNP' herein after. Especially, the 1:3 ratio combination of PAH/C-Oh-AuNP and PAH/PAA (Figure 6c) exhibited well-distributed Nano-Raspberry AuNPs and S-AuNP in the hybrid film with micro-wrinkled structure. This fine wrinkled film struc-ture makes the effectively increased surface area and the better contacts between spherical gold nanoparticles within PAH/PAA film with C-Oh-Au particles in PAH/C-Oh-AuNP film, making closely connected AuNPs. Inset of Figure 6(d) is the schematic view of the Nano-Raspberry AuNP. This extraordinary nanostructured AuNP exhibits much sharper and enhanced absorption peak compared to the conventional AuNP in UV spectrum (**Figure 5, 1a~c**).

We have tried TEM measurement of the PAH/C-Oh-AuNP films to define their structural characterization. However, TEM experiment was not suitable for the sophisticate and fragile polymer-AuNP film structure. The preparation, microtoming and transfer of the sample tends to damage the polymer film, so this process eventually distorted the polymer-AuNP hybrid film and changed it different from the originally assembled state. Therefore, we instead prepared C-Oh-AuNPs with the polymer thin film coating, $(PAH/PAA)_{3.5}$ film which is almost same as the hybrid coating with C-Oh-AuNPs we created on SPR chip. This $(PAH/PAA)_{3.5}$-coated C-Oh-AuNPs can be considered as the analog of $[(PAH/C\text{-}Oh\text{-}AuNP)_1+(PAH/PAA)_3]$, the sample in Figure 6(C). Then we measure SEM and TEM for these particles, the results were summarized in Supporting information (Figure S1).

Enhanced Biosensing Ability of the Nano-Raspberry AuNPs System

In the above section, we confirmed the enhanced bio-sensing ability of the C-Oh-AuNPs-hybrid film coated SPR chip compared to regular bare one. This enhanced signal might be increased with addition of AuNPs in the coating, however, there is a limit of the film thickness on a SPR chip due to the detectable reflectance and angle shift range. Therefore, the higher SPR intensity with the thinner film may be required. Since our Nano-Raspberry AuNP has a hierarchical protrusive structure of nanoparticles we expected the coating of Nano-Raspberry AuNPs would pre-sent enhanced surface plasmon resonance effect. Besides, the Nano-Raspberry AuNP has increased surface area to immobilize bioactive molecules such as antibody or anti-gen. To test the effect of the protrusive gold structure, we prepared a Nano-Raspberry AuNP coating on a SPR sensor chip. For comparison, we fabricated two different surface-coated SPR chips, one chip coated with $(PAH/C\text{-}Oh\text{-}AuNP)_2$ film (for comparison, denoted as uni-film) and the other one coated with (PAH/C-Oh-AuNP)+(PAH/PAA) mixed film to synthesize Nano-Raspberry AuNPs. We chose only one layer of C-Oh-AuNP in the mixed film while two layers were used in uni-film to keep the AuNP content of the mixed film system below than the C-Oh-AuNP system even after S-AuNP synthesis. Then this time we immobilized PSA antibodies, more specific biomarker to detect prostate cancer (**Figure 7**).

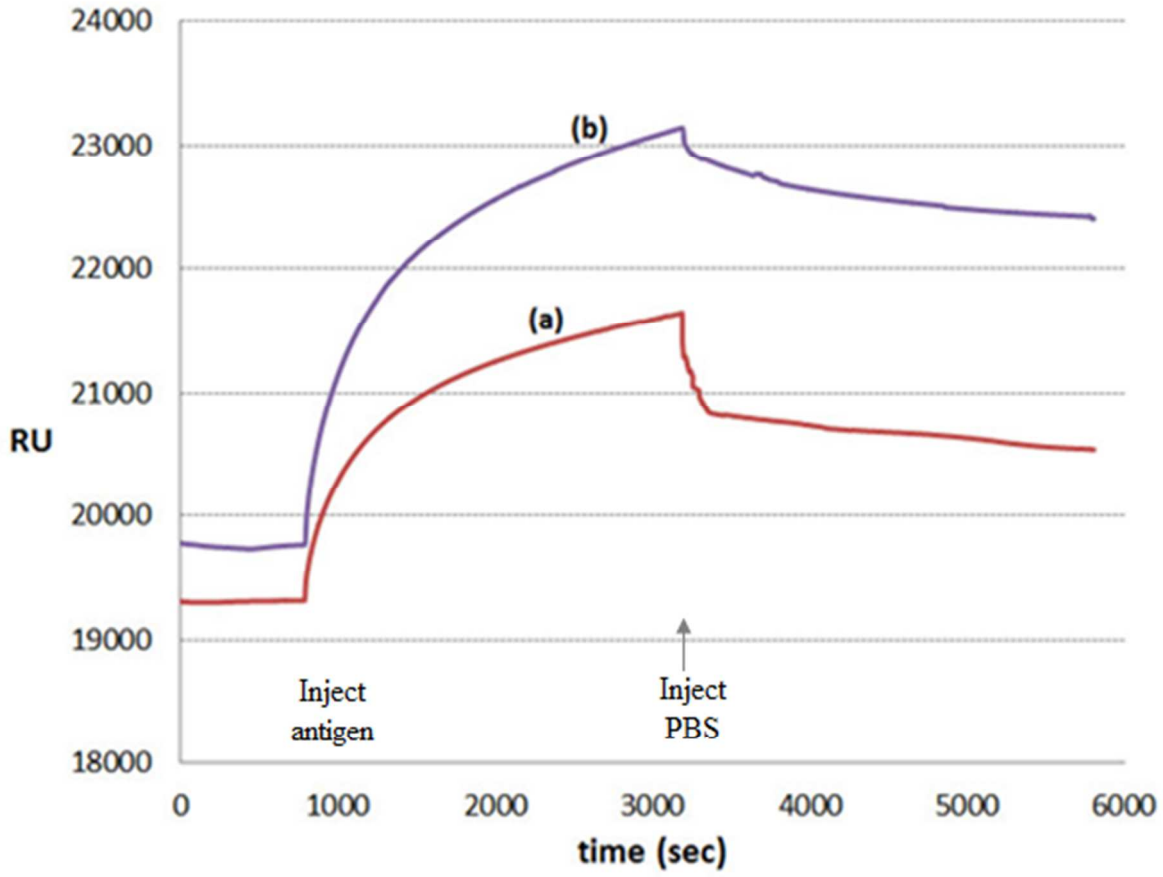

Figure 7. Real time mode multichannel SPR (BIAcore) sensograms of the AuNP-polyelectrolyte multilayer films, specifically anti-PSA immobilized on (a) $(PAH/C\text{-}Oh\text{-}AuNP)_2$ film and (b) S-AuNP-synthesized $[(PAH/C\text{-}Oh\text{-}AuNP)+(PAH/PAA)]_1$ coating for the detection of prostate specific antigen (PSA). Arrows indicate the injection points of antigen and PBS buffer solution. 1000 response units (RU) represent $1 ng/mm^2$.

The SPR chip coated with the raspberry-like hierarchical AuNP film (**Figure 7b**) presented more than twice greater binding signal ($\Delta RU \approx 2710$) than the C-Oh-AuNP only film ($\Delta RU \approx 1190$) (**Figure 7a**). This enhanced affinity might be due to the hierarchical AuNP structure which has the greater surface area with higher chemical functionality com-pared to just C-Oh-AuNP-only system. Using Nano-Raspberry AuNP coating will be a promising solution for the functional coating for SPR surface modification in which the film thickness has a limitation.

Micro-patterning of the AuNPs on atop of Antifouling Film for Fabrication of a Multi-Code Protein Sensor Chip

The assembled PAH/C-Oh-AuNP film was used to make a multi-code micro-patterned biosensor chip by introducing bioactive molecules conjugated on the nanoparticles through chemical functional groups. In order to create micro-patterns of AuNPs onto the chip, the PAH/PAA(3.0/3.0) film was chosen as the base coating which exhibited anti-fouling property. [28, 37] Antifouling is the ability of specifically designed materials and coatings to remove or block non-specific accumulation of proteins and cell on wetted surfaces, therefore maintaining chemical reactivity for bio-conjugation.[18, 38] Even though this base coating is very thin film (~10 nm), it behaves as excellent anti-fouling hydrogel so preventing non-reversible adsorption of proteins. On this PAH/PAA film a PAH ink used for microstamping, and the positive charged PAH-patterned surface attracted negative charged C-Oh-AuNPs through ionic bonding. Subsequent immobilization of proteins (biomarkers) on the patterned AuNPs was successfully performed by well-established thiol chemistry or amide conjugation depending on the functionality of the protein to introduce.

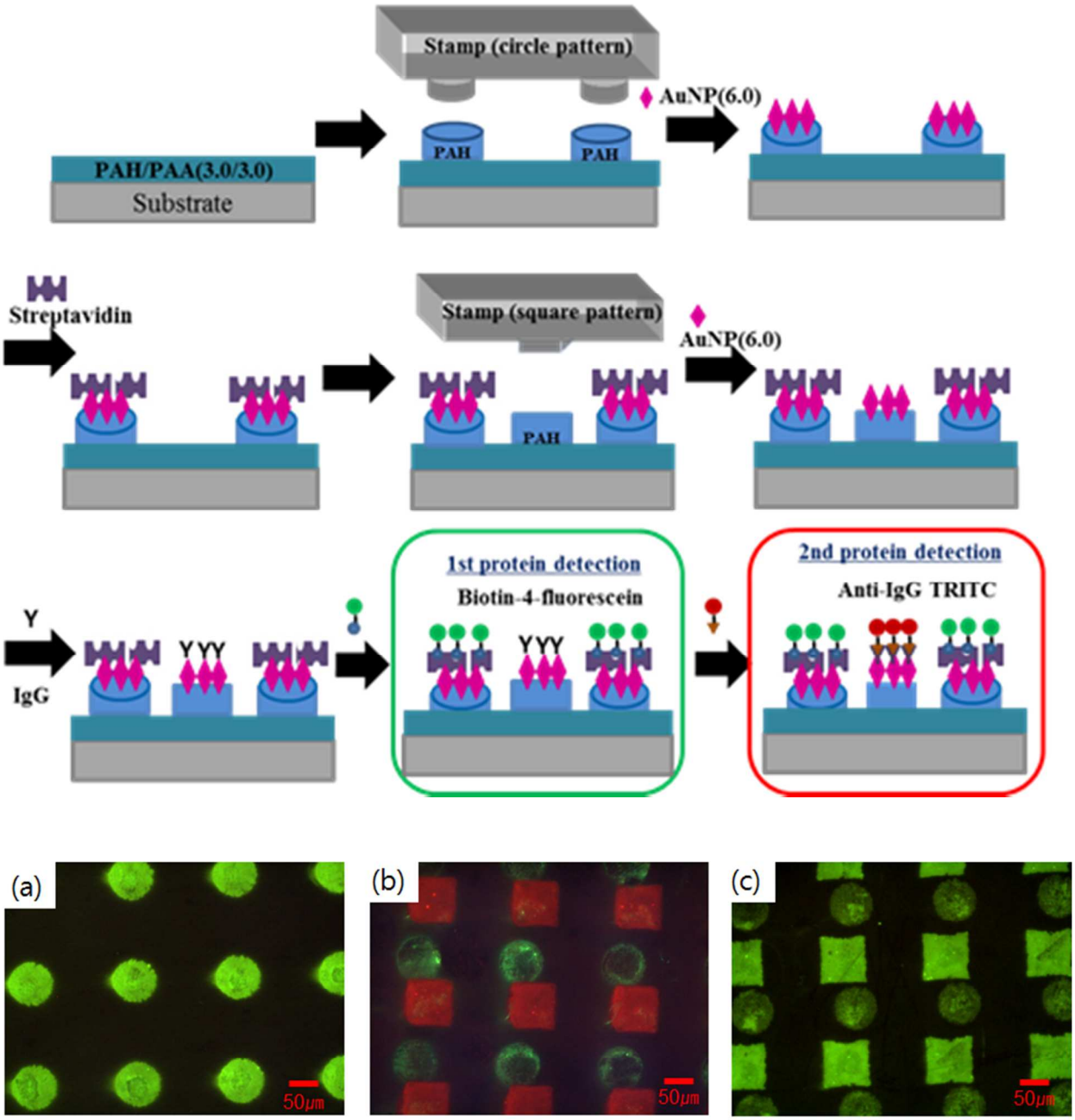

Figure 8. (Top) Schematic diagram of the use of the multi-code micro-patterned AuNP-polyelectrolyte multilayer film for detecting the model proteins biotin and anti-IgG. (Bottom) The dual-code fluorescent micro-array patterns of colors and shapes: (a) one-color one-shape (biotin, step A only), (b) dual-color (red and green) dual-shape (step A and B), (c) and one-color (step A and B for green label) dual-shape micro-patterned biochips.

Figure 8 shows the dual-shape and dual-colored signals that were activated by two different proteins. The chip on which IgG and streptavidin were immobilized successfully presented the binding signals of the corresponding antibodies. The model antibodies, biotin and anti-IgG labeled respectively with green and red fluorescent dyes, were applied on the patterns where the corresponding proteins immobilized indicating antibody-antigen binding.

At first, streptavidin was bound onto the surfaces of the C-Oh-AuNPs those were bound to the PAH micro-patterned areas. Then PAH was micro-stamped again on other spots on the chip, and it allowed the binding of new C-Oh-AuNPs atop of the new PAH patterns. Next, IgG was immobilized on the secondly micro-patterned C-Oh-AuNP-surfaces. Then, this dual patterned sample was exposed to biotin solution, successfully created the first antibody-immobilized patterns (**Figure 8a**). The following step was applying anti-IgG solution onto the IgG-immobilized area. To visualize each protein bound on the patterns, biotin and anti-IgG were labeled with red and green fluorescent dyes, i.e., FITC and TRICT, respectively **(Figure 8b**). It is possible for the two antibodies to be applied simultaneously. Since the colored patterns were very clearly and distinctively presented, we could confirm the antifouling property (i.e. blocking non-specific protein adsorption) of the AuNP/polyelectrolyte multilayer film as well as the base coating. This florescence labeling method is useful for the fast qualitative detection for multicomponent. At the same time, since our platform is active in SPR sensing, it is also able to sensing by more quantitative evaluation.

As noted above, we used such two-color-dyes to distinguish the binding proteins initially. But it is also possible to same dye for those antibodies, because using different shapes in the sequential micro-patterning allowed distinguishing of the bound proteins. It was proven as the result in **Figure 8c**, which was prepared with the same fluorescent dye (green dye) for two types of

proteins, still made us recognize each antigen-antibody binding. Since PAH/C-Oh-AuNP layers are readily formed either by LbL dipping or microstamping and the surface functional groups of the hybrid film are useful for further bio-conjugation, this system might be useful for biochip application contend with the limited choice of fluorescent dyes in the labeling process. Such a design might be especially useful for the case of signals having similar fluorescence intensities. In principle, by using more shapes on the patterns, more proteins can be applied on the chip.

CONCLUSION

In conclusion, we fabricated biochips that were gold chips coated with dual-patterned films where the bio-active component was immobilized on the patterned areas. The patterned areas were created with anisotropic gold-polymer hybrid film. Due to the high surface/volume ratio, we obtained relatively strong binding signals from the sensor chip coated with the hybrid film. We also created a hierarchical nanostructured AuNP system, spherical gold nanoparticles(S-AuNPs) attached onto a larger octahedral gold nanoparticle (C-Oh-AuNP), presenting "Nano-raspberry"-like shape which created by using the functionality of C-Oh-AuNP and PAH/PAA mixed layer film. In-situ gold nanoparticle synthesis was conducted on both C-Oh-AuNP and PAA in the multilayer film. The film exhibited highly enhanced sensitivity in bio-sensing experiments with even only one-layer coated sample. This hierarchical nano-protrusive AuNP system is a highly advantageous material for the sensitive and reliable bio-sensing system with the ability of micro-patterning. As an example, the use of different colors and shapes of patterned biological contents demonstrated here will provide more versatile application in sensing technologies.

AUTHOR INFORMATION

Corresponding Author

*sungyun@cnu.ac.kr

Author Contributions

The manuscript was written through contributions of all authors. All authors have given approval to the final version of the manuscript. §These authors contributed equally.

ACKNOWLEDGMENT

This work was supported by Chungnam National University fund and the National Research Foundation (NRF) funded by the Korean government through the Ministry of Science and ICT (MSIT) (No. 2017R1A2B4003578).

REFERENCES

(1) Nikoobakht, B.; El-Sayed, M. A., Preparation and growth mechanism of gold nanorods (NRs) using seed-mediated growth method. *Chem. Mater.*, **2003**, 15 (10), 1957-1962.

(2) Jin, R.; Cao, Y.; Mirkin, C. A.; Kelly, K.; Schatz, G. C.; Zheng, J., Photoinduced conversion of silver nanospheres to nanoprisms. **Science**, **2001**, 294 (5548), 1901-1903.

(3) Pingarrón, J. M.; Yáñez-Sedeño, P.; González-Cortés, A. Gold nanoparticle-based electrochemical biosensors. *Electrochimica Acta,* **2008**, 53 (19), 5848-5866.

(4) Qian, Z.; Park, S.-J. Silver seeds and aromatic surfactants facilitate the growth of anisotropic metal nanoparticles: gold triangular nanoprisms and ultrathin nanowires. *Chem. Mater*., **2014**, 26 (21), 6172-6177.

(5) Jiang, G.; Baba, A.; Ikarashi, H.; Xu, R.; Locklin, J.; Kashif, K. R.; Shinbo, K.; Kato, K.; Kaneko, F.; Advincula, R. Signal enhancement and tuning of surface plasmon resonance in Au nanoparticle/polyelectrolyte ultrathin films. *J. Phys. Chem. C*, **2007,** 111 (50), 18687-18694.

(6) Basiruddin, S. K.; Maity, A. R.;Saha, A.; Jana, N. R. Gold-Nanorod-Based Hybrid Cellular Probe with Multifunctional Properties. *J. Phys. Chem. C*, **2011**, *115*, 19612-19620.

(7) Liu, J.; Lu, Y. A colorimetric lead biosensor using DNAzyme-directed assembly of gold nanoparticles. *J. Am. Chem. Soc*., **2003**, 125 (22), 6642-6643.

(8) Ahmad, R.; Griffete, N.; Lamouri, A.; Felidj, N.; Chehimi, M. M.; Mangeney, C. Nanocomposites of Gold Nanoparticles@Molecularly Imprinted Polymers: Chemistry, Processing, and Applications in Sensors. *Chem. Mater*., **2015**, 27 (16), 5464-5478.

(9) Lee, S. J.; Park, G.; Seo, D.; Ka, D.; Kim, S. Y.; Chung, I. S.; Song, H. Coordination Power Adjustment of Surface□Regulating Polymers for Shaping Gold Polyhedral Nanocrystals. *Chem.-A European J.*, **2011**, 17 (30), 8466-8471.

(10) Lee, J.; Park, J. C.; Bang, J. U.; Song, H. Precise tuning of porosity and surface functionality in Au@ SiO2 nanoreactors for high catalytic efficiency. *Chem. Mater*., **2008,** 20 (18), 5839-5844.

(11) Peng, S.; McMahon, J. M.; Schatz, G. C.; Gray, S. K.; Sun, Y. Reversing the size-dependence of surface plasmon resonances. *Proc. Nat. Aca. Sci.,* **2010**, 107(33), 14530-14534.

(12) Huang, Y.; Wu, L.; Chen, X.; Bai, P.; Kim, D.-H. Synthesis of Anisotropic Concave Gold Nanocuboids with Distinctive Plasmonic Properties. *Chem. Mater.,* **2013**, 25 (12), 2470-2475.

(13) Hua, Y.; Chandra, K.; Dam, D. H. M.; Wiederrecht, G. P.; Odom, T. W. Shape-dependent nonlinear optical properties of anisotropic gold nanoparticles. *J. Phys. Chem. Letters*, **2015**, 6 (24), 4904-4908.

(14) Lohse, S. E.; Murphy, C. J., The quest for shape control: a history of gold nanorod synthesis. *Chem. Mater.* **2013,** 25 (8), 1250-1261.

(15) Schwartzkopf, M.; Buffet, A.; Körstgens, V.; Metwalli, E.; Schlage, K.; Benecke, G.; Perlich, J.; Rawolle, M.; Rothkirch, A.; Heidmann, B.; Herzog, G.; Müller-Buschbaum, P.; Röhlsberger, R.; Gehrke, R.; Stribeck N.; Roth, S. V. From atoms to layers: in situ gold cluster growth kinetics during sputter deposition *Nanoscale* **2013**, 5, 5053–62.

(16) Roth, S. V.; Santoro, G.; Risch, J. F. H.; Yu, S.; Schwartzkopf, M.; Boese, T.; Döhrmann, R.; Zhang, P.; Besner, B.; Bremer, P.; Rukser, D.; Rübhausen, M. A.; Terrill, N. J.; Staniec, P. A.; Yao, Y.; Metwalli, E.; Müller-Buschbaum, P. Patterned Diblock Co-Polymer Thin Films as Templates for Advanced Anisotropic Metal Nanostructures, *ACS Appl. Mater. Interfaces*, **2015**, 7 (23), 12470-12477.

(17) Schwartzkopf, M.; Hinz, A.; Polonskyi, O.; Strunskus, T.; Löhrer, F. C.; Körstgens, V.; Müller-Buschbaum, P.; Faupel, F.; Roth, S. V. Role of Sputter Deposition Rate in Tailoring Nanogranular Gold Structures on Polymer Surfaces, *ACS Appl. Mater. Interfaces*, **2017**, 9, 5629-5637.

(18) Jeong, H. J.; Pyun, W. H.; Yang, S. Y. Gold Nanoparticle□Hybridized Nano□Sponge Polymer Coatings to Enhance the Reliability and Sensitivity of Biosensors. *Macromol. Rapid Comm.*, **2009**, 30 (13), 1109-1115.

(19) Shin, N.-H.; Park, S.-H.; Lee, K.-H.; Yang, S. Y. Study of the platinum nanoparticle synthesis in polyelectrolyte multilayer films and their electrical and morphological surface properties. *Macromol. Res.*, **2013,** 21 (3), 302-305.

(20) Decher, G. Fuzzy nanoassemblies: toward layered polymeric multicomposites. *Science*, **1997**, 277 (5330), 1232-1237.

(21) Kotov, N. A.; Dekany, I.; Fendler, J. H. Layer-by-layer self-assembly of polyelectrolyte-semiconductor nanoparticle composite films. *J. Phys. Chem.,* **1995**, 99 (35), 13065-13069.

(22) Bertrand, P.; Jonas, A.; Laschewsky, A.; Legras, R. Ultrathin polymer coatings by complexation of polyelectrolytes at interfaces: suitable materials, structure and properties. *Macromol. Rapid Comm*., **2000**, 21 (7), 319-348.

(23) Johnston, A. P.; Cortez, C.; Angelatos, A. S.; Caruso, F. Layer-by-layer engineered capsules and their applications. *Current Opinion in Colloid & Interface Science,* **2006**, 11 (4), 203-209.

(24) Yang, S. Y.; Rubner, M. F. Micropatterning of polymer thin films with pH-sensitive and cross-linkable hydrogen-bonded polyelectrolyte multilayers. *J. Am. Chem. Soc*., **2002**, 124 (10), 2100-2101.

(25) Kozlovskaya, V.; Ok, S.; Sousa, A.; Libera, M.; Sukhishvili, S. A. Hydrogen-bonded polymer capsules formed by layer-by-layer self-assembly. *Macromolecules* **2003**, 36 (23), 8590-8592.

(26) Yang, S. Y.; Lee, D.; Cohen, R. E.; Rubner, M. F. Bioinert solution-cross-linked hydrogen-bonded multilayers on colloidal particles. *Langmuir* **2004**, 20 (14), 5978-5981.

(27) Chapman, P.; Ducker, R. E.; Hurley, C. R.; Hobbs, J. K.; Leggett, G. J. Fabrication of two-component, brush-on-brush topographical microstructures by combination of atom-transfer radical polymerization with polymer end-functionalization and photopatterning. *Langmuir* **2015,** 31 (21), 5935-5944.

(28) Berg, M. C.; Yang, S. Y.; Hammond, P. T.; Rubner, M. F. Controlling mammalian cell interactions on patterned polyelectrolyte multilayer surfaces. *Langmuir* **2004**, 20 (4), 1362-1368.

(29) Kane, R. S.; Takayama, S.; Ostuni, E.; Ingber, D. E.; Whitesides, G. M., Patterning proteins and cells using soft lithography. In *The Biomaterials: Silver Jubilee Compendium*, Elsevier: **2006**; pp 161-174.

(30) Cha, S. H.; Lee, H. J.; Koh, W.-G. Study of myoblast differentiation using multi-dimensional scaffolds consisting of nano and micropatterns. *Biomater. Res.,* **2017**, 21 (1), 1.

(31) Glaser, R. H.; Wilkes, G. L. Structure property behavior of polydimethylsiloxane and poly (tetramethylene oxide) modified TEOS based sol-gel materials. *Polymer Bulletin* **1988,** 19 (1), 51-57.

(32) Yang, S. Y.; Kim, D. Y.; Jeong, S. M.; Park, J. W. Stimuli□Responsive Hybrid Coatings of Polyelectrolyte Multilayers and Nano□Patterned Polymer Brushes. *Macromol. Rapid Comm.,* **2008,** 29 (9), 729-736.

(33) Park, J.-H.; Yang, S. Y. Colloidal particle assembly using micro-patterning onto morphology-controlled anti-fouling polyelectrolyte multilayer films. *Macromol. Res.,* **2016,** 24 (2), 98-98.

(34) Chia, K.-K.; Cohen, R. E.; Rubner, M. F. Amine-rich polyelectrolyte multilayer nanoreactors for in situ gold nanoparticle synthesis. *Chem. Mater.,* **2008**, 20 (21), 6756-6763.

(35) Cho, J.; Caruso, F. Investigation of the interactions between ligand-stabilized gold nanoparticles and polyelectrolyte multilayer films. *Chem. Mater.,* **2005,** 17 (17), 4547-4553.

(36) Kidambi, S.; Dai, J.; Li, J.; Bruening, M. L. Selective hydrogenation by Pd nanoparticles embedded in polyelectrolyte multilayers. *J. Am. Chem. Soc.,* **2004**, 126 (9), 2658-2659.

(37) Mendelsohn, J. D.; Yang, S. Y.; Hiller, J. A.; Hochbaum, A. I.; Rubner, M. F. Rational design of cytophilic and cytophobic polyelectrolyte multilayer thin films. *Biomacromolecules* **2003**, 4 (1), 96-106.

(38) Lee, M. H.; Hribar, K. C.; Brugarolas, T.; Kamat, N. P.; Burdick, J. A.; Lee, D. Harnessing interfacial phenomena to program the release properties of hollow microcapsules. *Adv. Func. Mater*. **2012**, 22 (1), 131-138.

Table of Contents